

NASA Technical Memorandum 4148

**Flutter Clearance of the F-18
High-Angle-of-Attack Research
Vehicle With Experimental
Wingtip Instrumentation Pods**

Lawrence C. Freudinger

OCTOBER 1989

NASA

NASA Technical Memorandum 4148

**Flutter Clearance of the F-18
High-Angle-of-Attack Research
Vehicle With Experimental
Wingtip Instrumentation Pods**

Lawrence C. Freudinger
Ames Research Center
Dryden Flight Research Facility
Edwards, California



National Aeronautics and
Space Administration
Office of Management
Scientific and Technical
Information Division

1989

SUMMARY

An F-18 aircraft was modified with wingtip instrumentation pods for use in NASA's high-angle-of-attack research program. Ground vibration and flight flutter testing were performed to clear an acceptable flight envelope for the aircraft. Flight test utilized atmospheric turbulence for structural excitation; the aircraft displayed no adverse aeroelastic trends within the envelope tested. The data presented in this report include mode shapes from the ground vibration tests and estimates of frequency and damping as a function of Mach number.

NOMENCLATURE

<i>c.g.</i>	center of gravity
<i>G</i>	structural damping factor (2 percent $G = 1$ percent viscous damping ratio)
<i>g</i>	acceleration of gravity (1 $g = 32.2$ ft/sec ²)
HARV	high-angle-of-attack research vehicle
KCAS	knots calibrated airspeed
KEAS	knots equivalent airspeed
GVT	ground vibration test
kft	kilofeet (1 kft = 1000 ft)

INTRODUCTION

Structural modifications to research aircraft are a common occurrence in many flight research projects at NASA, and caution must be exercised to prevent these modifications from adversely affecting the aeroelastic characteristics of the aircraft. Avoiding or preventing the occurrence of flutter (and maintaining flight safety in general) is given high priority for one-of-a-kind research aircraft. The F-18A high-angle-of-attack research vehicle (HARV) is part of NASA's high alpha technology program which is an effort to accelerate the development of key technologies applicable to increasing the effectiveness of fighter aircraft designs. The key technologies include the aerodynamics of separated and vortical flow, maneuver management, and propulsive control. Phase I of this program required the addition of instrumentation pods on each wingtip designed to house cameras and to provide structural support for air data probes. These pods replaced the missile launcher rails normally found on the aircraft wingtips.

A predictive vibration and flutter analysis was performed that resulted in recommended restrictions to the flight envelope. Also, a quick-look experimental frequency check of the aircraft with the pods installed revealed significant anomalies in the symmetric and antisymmetric first torsion mode frequencies relative to the predicted values. Because these frequency shifts were unexplained and their effects on the flutter speed were unknown, it was decided that a flight flutter test be performed to verify that the aircraft was indeed free from flutter within a useable envelope. In preparation for the flight test, a ground vibration test (GVT) was performed to accurately identify mode shapes for comparison to the analyses and the unmodified aircraft. This report includes measured mode shapes from the GVT and frequency and damping estimates from the flight test as a function of Mach number.

VEHICLE DESCRIPTION

The F-18A (Ship #F-6, Bureau #160780, NASA 840) is a preproduction single-seat fighter/attack aircraft powered by two F-404-GE-400 turbofan engines with afterburners and fixed inlets. The wings feature hydraulically actuated leading and trailing edge flaps and ailerons, as well as wingtip folds for aircraft carrier operation. The folds, however, were locked in the down position for the duration of the research program. Twin vertical stabilizers, full-flying horizontal stabilizers, and wing leading edge extensions are among the other features of this aircraft

(fig. 1). The unique modification to the aircraft is the replacement of the AIM-9 missile launcher rails with instrumentation pods designed to house cameras and support wingtip air data sensors for high-angle-of-attack research. A two-view drawing of the left pod is shown in figure 2. The pods are approximately 30 percent lighter than the launcher rails they replaced but have an approximately 10 percent higher pitch inertia. Also, the center of gravity (*c.g.*) for the instrumentation pods is approximately 12.9 in. forward of the *c.g.* of the missile launcher rails.

GROUND VIBRATION TEST PROCEDURE

A GVT was required to identify structural frequencies and mode shapes for comparison with the analysis. The aircraft was supported on its gear with the struts deflated to minimize nonlinearities. Tire pressure was reduced to one-half operating pressure to lower the rigid body frequencies. Testing was accomplished with the fully fueled aircraft's electrical and hydraulic systems operating.

The objectives of the GVT were

1. to measure the frequencies of the major aircraft structural modes below 25 Hz,
2. to measure the mode shapes of the first four wing modes and the primary mode shapes involving the horizontal and vertical tail surfaces,
3. to assess predictive analysis accuracy by comparing measured modal data with predicted data, and
4. to investigate the sensitivity of the torsion frequencies to instrument pod mass and *c.g.* location.

Instrumentation

Piezoelectric accelerometers were attached to the aircraft to measure its dynamic response. Force links were used to measure the input forces from the two electrodynamic shakers. A minicomputer-based structural analysis system (fig. 3) was used to acquire and analyze 129 structural locations in sets of six.

Excitation

Multi-input, uncorrelated, random excitation was used for the initial modal survey (Vold and Rocklin, 1982; Hunt and Peterson, 1983; General Electric, 1983; Kehoe, 1987). Sine dwell was used for an investigation of pod inertia effects and for when random excitation proved unable to adequately excite some of the modes in the upper half of the frequency range of interest (Kehoe, 1987). Shakers were placed at each wingtip at the rear spar. This choice of shaker location was adequate for exciting all of the wing modes of interest with the exception of the second wing bending modes, whose shakers were moved to the front spar near the wing fold. Frequency sweeps were performed first to obtain a cursory look at resonant frequencies and for preliminary comparison with the manufacturer's GVT data. For brevity, these frequency sweeps are not presented here.

Fifty-pound preloads were applied to the leading edge flaps to reduce the nonlinearities caused by freeplay in the flap hinges. These preloads were suspended by an amount of elastic cord so that the plunge frequency of the preload was well below the first elastic mode of the aircraft. A typical plunge frequency was approximately 0.9 Hz. A photograph of the use of these preloads on the left outboard leading edge flap is shown in figure 4.

Structural Mode Measurements

Response data from the random excitation were acquired, averaged, and then stored in the frequency domain. The data were sampled at 128 samples/sec into blocks of 1024 samples with the antialiasing filters set at 50 Hz. A Hanning window was applied to each block to reduce leakage errors. After fifty averages of data were acquired for the aircraft, the modal parameters were estimated with a multiple-input time domain method known as polyreference (Vold and Rockin, 1982; Hunt and Peterson, 1983; General Electric, 1983).

In addition to the procedures already discussed, the pod weight and *c.g.* were subsequently changed to match those of a standard AIM-9 missile launcher rail by temporarily placing 25 lb of lead shot 28.8 in. aft of the forward mounting bolt. Sinusoidal excitation was then used to tune in both the symmetric and antisymmetric torsion modes again in order to observe the effect of the weight and *c.g.* change of the wingtip fixture on the torsion mode frequencies.

FLIGHT TEST PROCEDURE

The objective of the flight test was to verify freedom from flutter within an envelope not to exceed Mach 2.0 below 730 knots calibrated airspeed (KCAS). Frequency and damping values were estimated and are shown for the four lowest elastic modes only.

Flight flutter testing was conducted at altitudes of 34,000, 15,000, and 5000 ft. Also, an envelope sweep (high-speed dive) was planned to demonstrate freedom from flutter at speeds beyond those which were attainable through level flight acceleration. Clearing the envelope to the standard aircraft configuration maximum speed placard of 730 KCAS was not realistic because of the aircraft's level flight thrust limitations. Thus, the speed at which the dive maneuver was to be performed was determined by the results of the constant altitude portion of the flight test.

The subsonic envelope was cleared first, followed by the transonic, and subsequently the supersonic regime (fig. 5). Windup turns were accomplished at typically every odd-numbered tenth of a Mach number being tested in order to observe any sensitivity to angle of attack.

Instrumentation

Piezoelectric accelerometers were used to monitor the dynamics of the structure. The transducer locations for the flight test are shown in figure 6. Velocity and altitude information was obtained from standard National Advisory Committee for Aeronautics noseboom and aircraft instrumentation. Digital telemetry was used to transmit the information to the ground where it was displayed in real time in both the frequency and time domain.

Excitation

Random atmospheric turbulence and pilot-generated control surface pulses were used as excitation to the structure because an in-flight excitation system was not available. One minute of stabilized data was collected at each test point followed by a control surface pulse in each of the three body axis directions. The signal-to-noise ratio observed is typically low when using natural turbulence to excite the structure, and it is expected that some data points will have to be repeated or discarded.

Envelope Clearance Procedure

The aircraft was slowly accelerated (2 to 4 knots/sec) to the specified Mach number at the test altitude. Slow acceleration is a standard precaution and is utilized by the test engineers to observe the stripchart traces for adverse

behavior. Experience has shown that an unstable mechanism may catastrophically diverge in only a few cycles of oscillation, which leaves little time to terminate the maneuver. Once the aircraft was stabilized at the new test point, 60 sec of data were acquired followed by a series of three control surface pulses. At specified test points (typically every other test point), the aircraft then performed a constant altitude windup turn to observe the aircraft's behavior at increased angle of attack.

Telemetered data were displayed on strip charts and spectral analyzers in the ground station. Because it was known that two of the critical wing modes—one symmetric mode and one antisymmetric mode—were very close in frequency, wingtip acceleration traces were added and subtracted to clarify and distinguish those closely spaced modes. The usefulness of adding and subtracting data channels to separate closely spaced modes is revealed in figure 7, which shows how this manipulation of the left and right wingtip accelerometer traces have helped to distinguish two modes separated by less than 1 Hz.

All data channels were band-pass filtered with upper and lower cutoff frequencies of 40 Hz and 2 Hz, respectively. The data were acquired by a Fourier analyzer at 100 samples/sec into data blocks of 1024 samples, thus providing sufficient information for six averages at each test point. The Fourier analyzer was then used to calculate estimates of frequency and damping of critical modes in near-real time, and the same algorithms were used between flights to analyze all the modes of interest. This analysis consisted of calculating the autospectrum for each time history to extract estimates of frequency and damping by way of a single-degree-of-freedom frequency-domain curve fit (Soovere, 1975; Clough and Penzien, 1975; Kehoe, 1988). Clearance to proceed to the next test point came after the data was analyzed and the frequency and damping trends were extrapolated to the next test point and were considered to be satisfactory.

RESULTS AND DISCUSSION

Ground Vibration Test Results

The rigid body rotational modes of the aircraft supported on its landing gear were measured and are shown in table 1. Strong coupling between the rigid body modes was observed. This coupling was considered to be due to this particular aircraft's landing gear configuration, which made separation of the rigid body modes somewhat difficult.

Table 1 also compares the frequency and damping values of the modified aircraft with a standard launcher rail configuration. The values for the standard launcher rail configuration were measured in a separate but similar test. Note that random excitation techniques could not excite the 16.11 Hz and the 15.73 Hz modes, and the sine dwell method was subsequently chosen to extract the modal characteristics for these modes.

Figure 8 shows the resulting mode shapes for symmetric first wing bending and torsion modes and compares them to the corresponding mode shapes for the same aircraft with the standard launcher rails attached. The correlation for first symmetric bending between the two aircraft configurations is excellent. The torsion mode, on the other hand, displays a somewhat dramatic change in the wing displacement shape. With the instrumentation pods attached to the wing, the torsion mode displays a simple torsion shape, whereas the standard configuration possesses a more complex shape. This difference in shape may be attributed to a decrease in modal coupling in the modified aircraft corresponding to an additional 2-Hz spread between first wing torsion and second wing bending.

Figure 9 shows the resulting mode shapes for antisymmetric first wing bending and torsion modes and compares them to the corresponding mode shapes for the same aircraft with the standard launcher rails attached. As with the symmetric case, the first wing bending mode is not noticeably affected by the instrumentation pods. The torsion mode in this case is again different, but the differences are primarily in the horizontal and vertical stabilizers and not in the wings, as in the symmetric case. Specifically, the torsion mode for the modified aircraft displays a decrease in vertical stabilizer amplitude and the phase of the horizontal stabilizers is reversed. Again, these differences may be caused by the frequency of the torsion mode relative to other structural modes. The reversed phase of the horizontal

stabilizers indicates the presence of a stabilizer mode between 14.85 Hz and 12.29 Hz, and it was, in fact, measured at 13.59 Hz (table 1).

Table 1. Ground vibration test results.

F-18 ship F-6 GVT modal data				
Measured mode	With wingtip instrumentation pods		With standard launcher rails	
	Frequency, Hz	Structural damping ratio	Frequency, Hz	Structural damping ratio
Rigid body modes:				
Rigid body pitch	2.05	—	—	—
Rigid body roll	3.19	—	—	—
Symmetric modes:				
Wing first bending	6.05	0.028	5.94	0.020
Fuselage first bending	—	—	9.57	0.031
Wing first torsion	11.85	0.025	13.81	0.030
Wing second bending	16.11	0.048	16.59	0.042
Antisymmetric modes:				
Wing first bending	8.78	0.049	8.82	0.039
Fuselage first bending	8.22	0.080	8.49	0.042
Wing first torsion	12.29	0.030	14.85	0.039
Horizontal tail bending	13.59	0.062	13.60	0.037
Wing second bending	15.73	0.035	15.87	0.043

These relatively significant changes in the frequencies and mode shapes for the torsion modes were not predicted in the original analysis, and it was noted that the original (unpublished) vibration analyses supplied by the manufacturer modeled the stabilizer surfaces by point masses only. Including the tail surfaces in a final vibration analysis resulted in improving the correlation between analytical and measured frequencies and mode shapes. The analytical symmetric and antisymmetric torsion mode shapes are shown in figures 10 and 11.

A final predictive flutter analysis was performed by the manufacturer using the full aircraft finite element model (all tail surfaces and flexible wingtip pods included) to assess how the mode shapes and frequencies of the final vibration analysis would affect the predicted flutter speed. The results with the flexible empennage indicated an antisymmetric flutter speed of 825 KEAS, or 8 percent lower than the original analysis.

The experimental investigation into mass effects of the pod showed that the lowering of the torsion frequencies was not due to the differences in weight or *c.g.* between the pod and the standard launcher rail. No appreciable change in torsion frequencies was observed by the addition of 25 lb of lead shot 28.8 in. aft of the forward mounting bolt. Thus, the actual cause of the discrepancy is still unknown, although a possible explanation may be a change in wingtip boundary conditions due to the reduced stiffness of the pod (about one-third as stiff as the standard launcher rail).

Flight Test Results

Figures 12 and 13 show the flight test results for the four lowest elastic modes. Figure 12 shows the frequency and damping trends for the symmetric bending-torsion flutter mechanism for each of the three test altitudes. Note that on some plots frequency and damping values are missing. These data could not be extracted due to the lack of adequate excitation at these test points. Higher frequency modes were monitored but are not shown here because

they are not considered critical in the flutter mechanism. In addition, the higher frequency modes were more difficult to excite with atmospheric turbulence which decreased the reliability of the damping estimate. All data indicate satisfactory damping levels ($> 0.03G$, MIL-A-008870A) and trends for the symmetric flutter mechanism within the envelope tested.

Figure 13 shows the frequency and damping trends corresponding to the antisymmetric bending and torsion modes. In general, the data display some scatter, but trends are distinguishable in most of the plots. Classical transonic "dips" in the damping trends can be observed in most of the antisymmetric data, although it is interesting to note that, for a given mode, there are differences in the location of the transonic dip and at times a slight increase in damping in the high subsonic regime. All data indicate satisfactory damping levels and trends for the antisymmetric modes within the envelope tested.

Another interesting phenomenon was observed during testing at 34,000 ft. Figure 14 shows a waterfall plot of frequency response as a function of Mach at 34,000 ft for the left vertical stabilizer tip and the effect of supersonic flow on what appears to be the rudder rotation frequency. Maximum amplitude of the rudder vibration occurred at approximately Mach 1.3. An inspection of both rudders revealed excessive freeplay in the left actuator mechanism which resulted in the actuator's replacement. Subsequent observation showed a satisfactory increase in rudder damping. This phenomenon has been observed in previous programs with different aircraft at NASA (Kehoe, 1984).

The flutter clearance testing by way of stabilized points terminated short of the original envelope limit for the aircraft because the aircraft was thrust limited. Damping trends indicated adequate stability margin for a dive maneuver at 670 KCAS, which was successfully performed to demonstrate the absence of aeroelastic instabilities at that speed. The choice of 670 KCAS was chosen in part because of an additional aircraft placard at 670 KCAS below 8000 ft. Consequently, 670 KCAS was determined to be an acceptable limit for the research aircraft.

Figure 15 shows a summary of the completed stabilized points and outlines the Mach and altitude conditions during the intended 670 KCAS envelope sweep. Stabilized points, which included a windup turn to observe angle-of-attack effects, are indicated by a different symbol as shown. No adverse sensitivity to angle of attack was observed in any of the 2-g windup turns. The highest airspeed reached during the dive was 683 KCAS at approximately 27,000 ft. Strip chart traces indicated that structural stability was consistent with extrapolations from stabilized point data, and no further evaluation of the dive information was considered necessary.

Figure 16 shows the cleared flutter envelope for the aircraft, which is 670 KCAS or Mach 1.8, whichever is lower. The envelope represents more of the level flight capabilities of the aircraft than it does a known flutter boundary. Based on the predicted flutter speed, the flutter margin for these limits is no less than 20 percent.

CONCLUSIONS

An F-18 aircraft was modified with wingtip instrumentation pods for use in NASA's high-angle-of-attack research program. Ground vibration and flight flutter testing were performed to clear an acceptable flight envelope for the research program. No adverse aeroelastic trends were observed within the envelope tested.

The replacement of missile launcher rails with instrumentation pods lowered the torsion frequencies of the wing by 2 Hz. The specific reason or reasons that the instrumentation pods lowered the wing torsion frequencies were not determined. However, it was determined that differences in weight and center of gravity between the pod and a standard AIM-9 missile launcher rail had no significant effect.

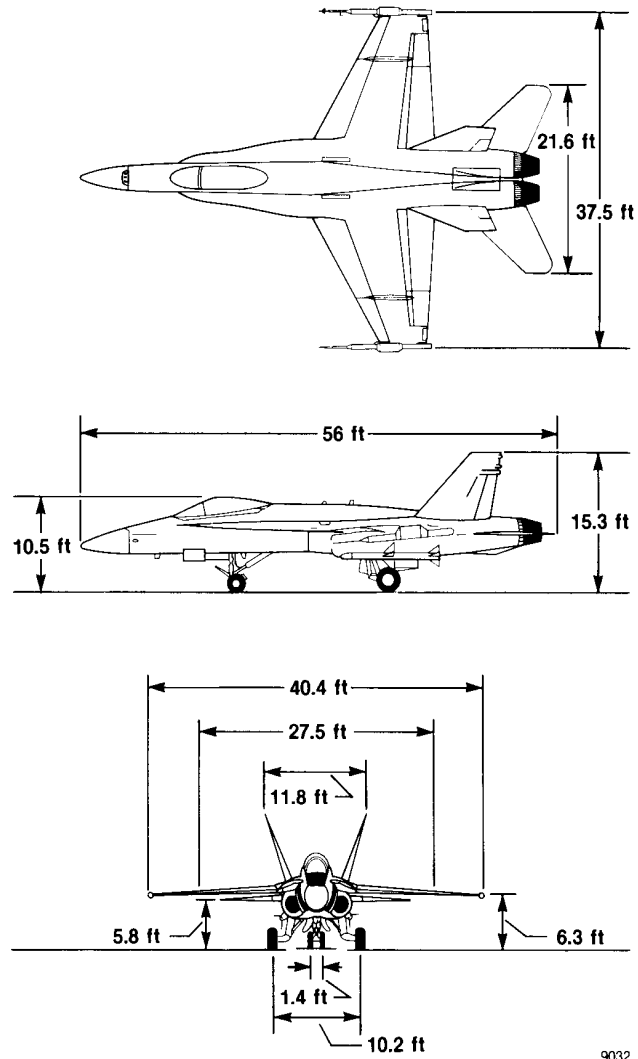
Measured mode shapes revealed a significant coupling of the horizontal and vertical stabilizer surfaces with the wings. The tail surfaces were modeled as point masses in the original analyses. Including all surfaces in the finite element analysis improved correlation with measured modal data. Flutter analyses using the full finite element model indicated an 8-percent reduction in flutter speed. The aircraft was successfully cleared to 670 knots calibrated airspeed below Mach 1.8.

Flight test revealed a lightly damped oscillation of the left rudder that was attributed to excessive freeplay in the left rudder actuator assembly. The assembly was subsequently replaced and the damping was significantly improved.

*Ames Research Center
Dryden Flight Research Facility
National Aeronautics and Space Administration
Edwards, California, November 29, 1988*

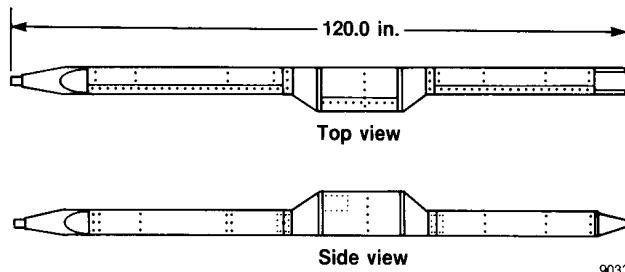
REFERENCES

- Clough, Ray W. and J. Penzien, *Dynamics of Structures*, ch. 4, McGraw-Hill, 1975.
- Hunt, David L. and Edward L. Peterson, *Multishaker Broadband Excitation for Experimental Modal Analysis*, SAE paper 83-1435, 1983.
- Kehoe, M.W., *Aircraft Flight Flutter Testing at the NASA Ames-Dryden Flight Research Facility*, AIAA paper 88-2075, May 1988.
- Kehoe, M.W., *Aircraft Ground Vibration Testing at NASA Ames-Dryden Flight Research Facility*, NASA TM-88272, 1987.
- Kehoe, M.W., *Highly Maneuverable Aircraft Technology (HiMAT) Flight Flutter Test Program*, NASA TM-84907, 1984.
- Soovere, J., *Turbulence Excited Frequency Domain Damping Measurement and Truncation Effects*, NASA SP-415, 1975, pp. 115–141.
- User Manual for Modal Analysis 8.0*, General Electric CAE International, 1983.
- Vold, H. and G.T. Rocklin, "The Numerical Implementation of a Multiple-Input Modal Estimation Method for Mini-computers," *International Modal Analysis Conference Proceedings*, Nov. 1982.



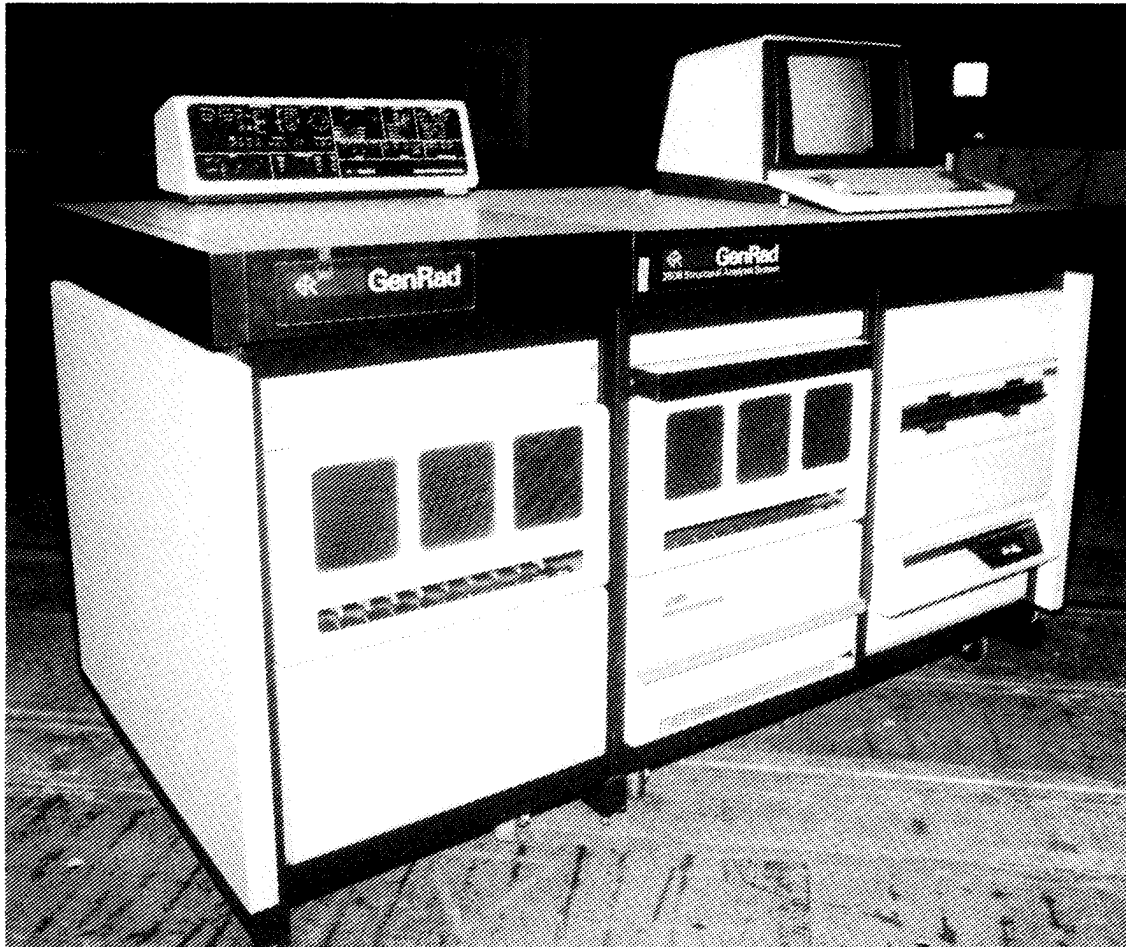
9032

Figure 1. High-angle-of-attack research aircraft (HARV).



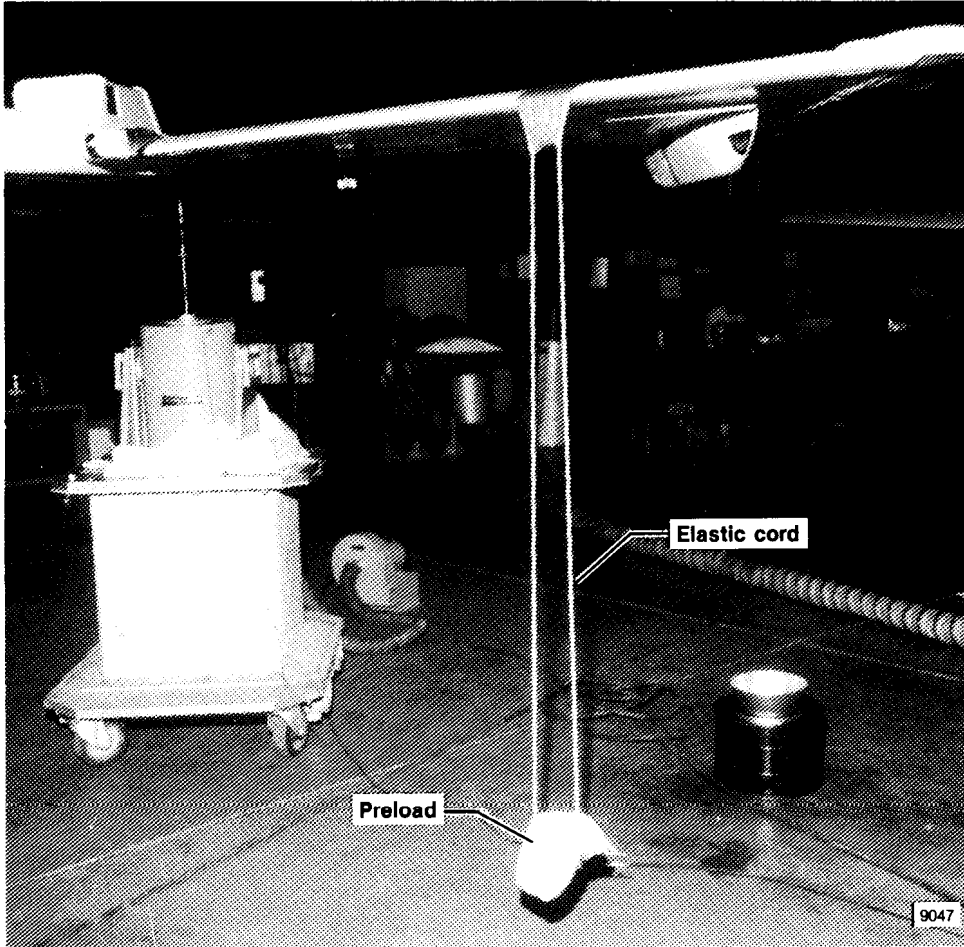
9033

Figure 2. Left instrumentation pod.



EC 87 0213-004

Figure 3. Minicomputer-based structural analysis system.



EC 87 0020-004

Figure 4. Ground vibration test setup showing use of preloads.

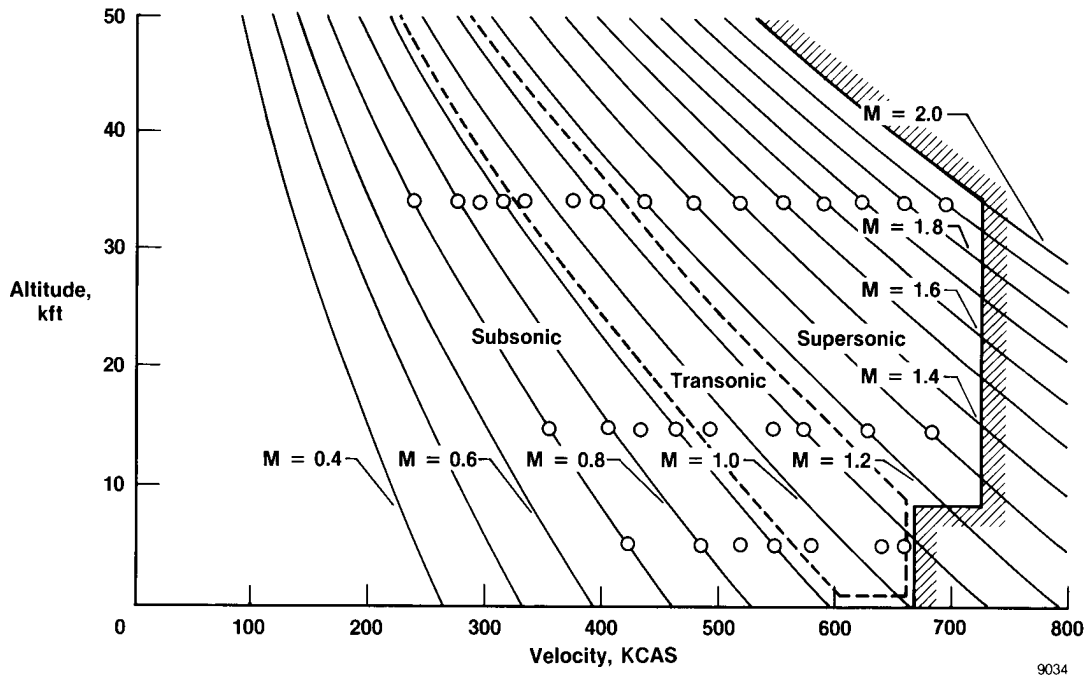
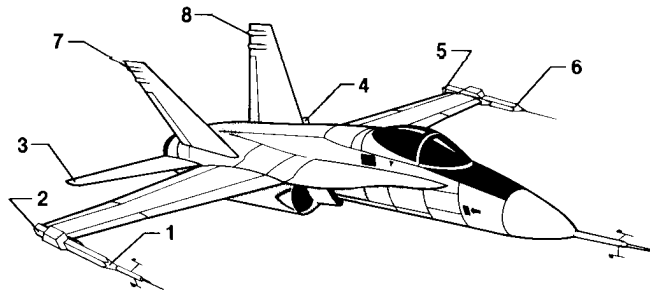


Figure 5. Planned flight test conditions.



Parameters	Range, G
1. Right wing forward normal accelerometer	± 10
2. Right wing aft normal accelerometer	± 10
3. Right horizontal tail normal accelerometer	± 25
4. Left horizontal tail normal accelerometer	± 25
5. Left wing aft normal accelerometer	± 10
6. Left wing forward normal accelerometer	± 10
7. Right fin lateral accelerometer	± 25
8. Left fin lateral accelerometer	± 25

9035

Figure 6. Flight test instrumentation locations.

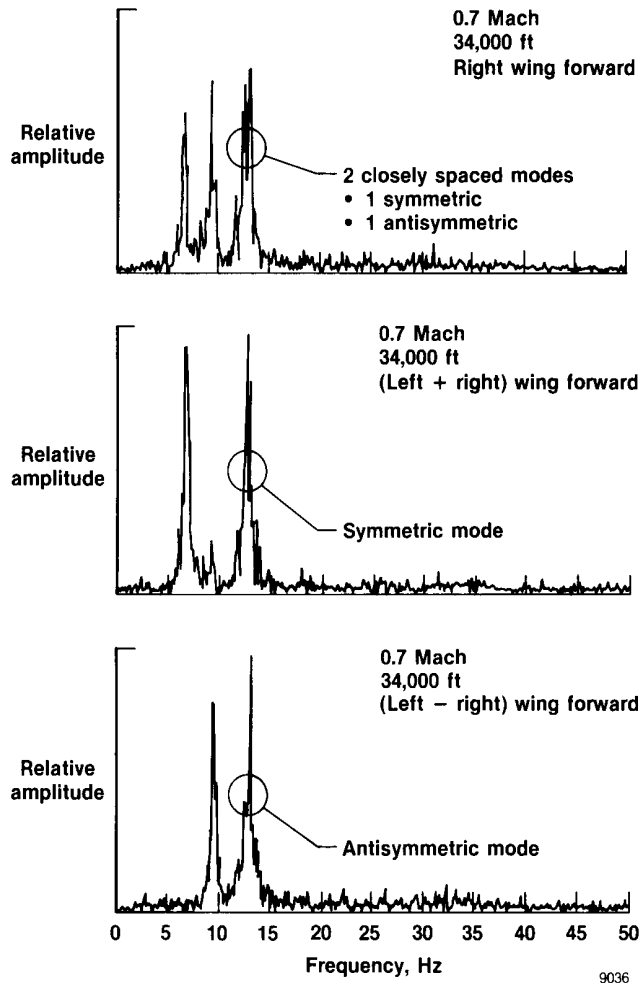
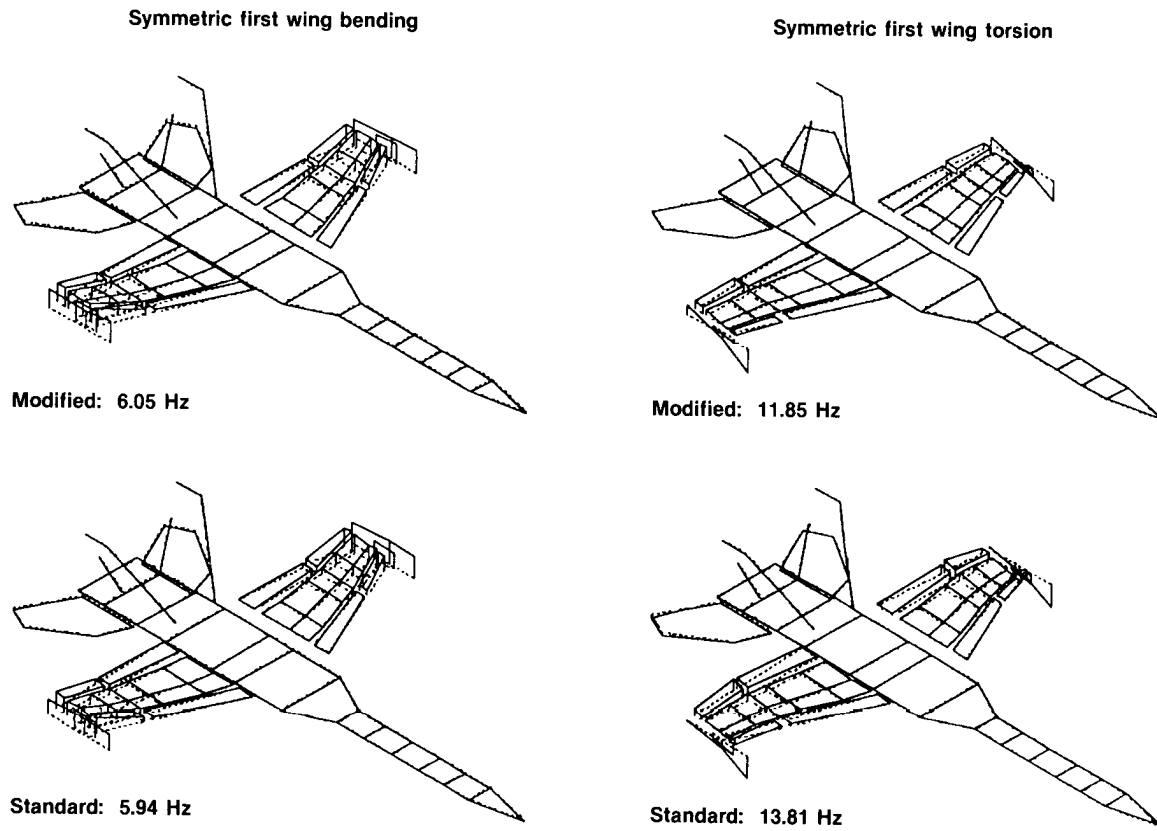


Figure 7. Example of data showing addition and subtraction of channels.



9037

Figure 8. Comparison of symmetric mechanism-measured mode shapes — instrumentation pods (modified) as opposed to launcher rails (standard).

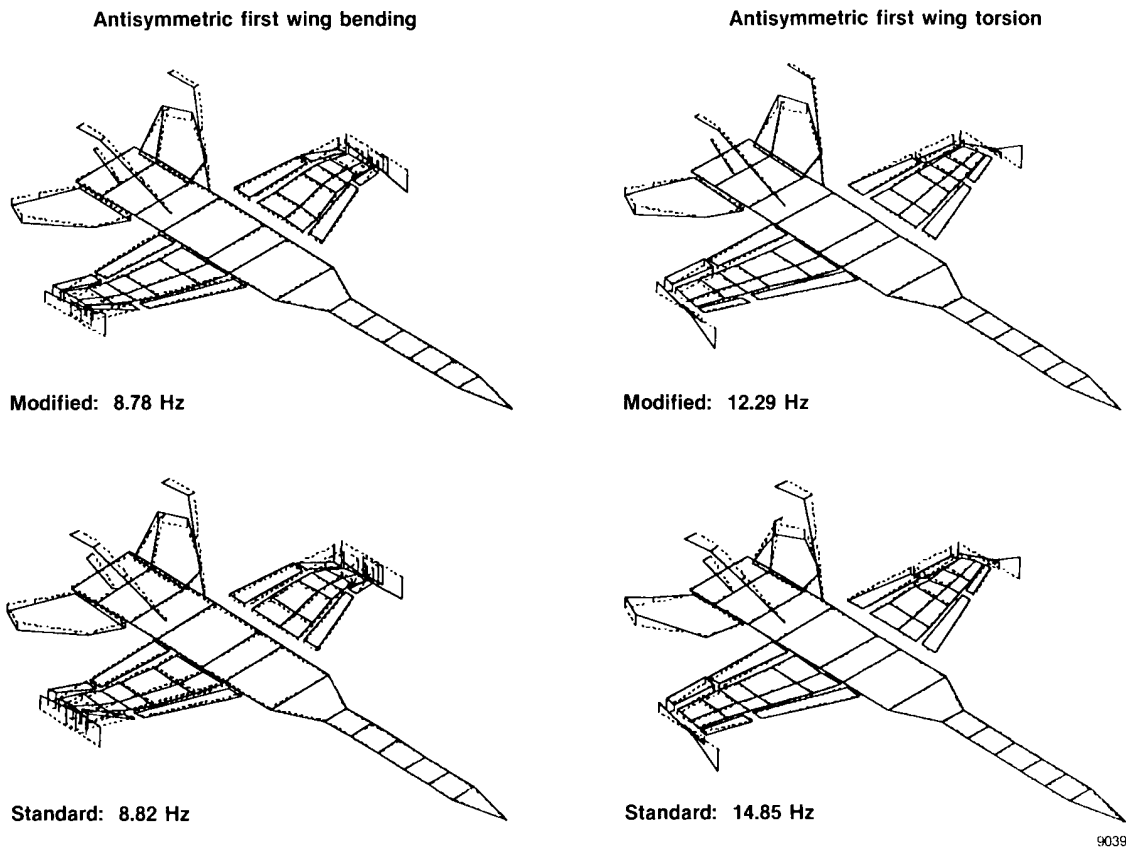


Figure 9. Comparison of antisymmetric mechanism-measured mode shapes — instrumentation pods (modified) as opposed to launcher rails (standard).

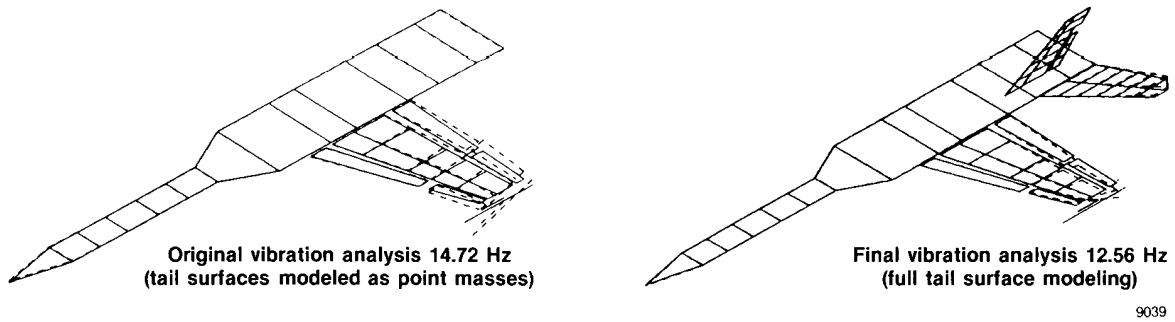


Figure 10. Analytical mode shape comparison — symmetric first wing torsion.

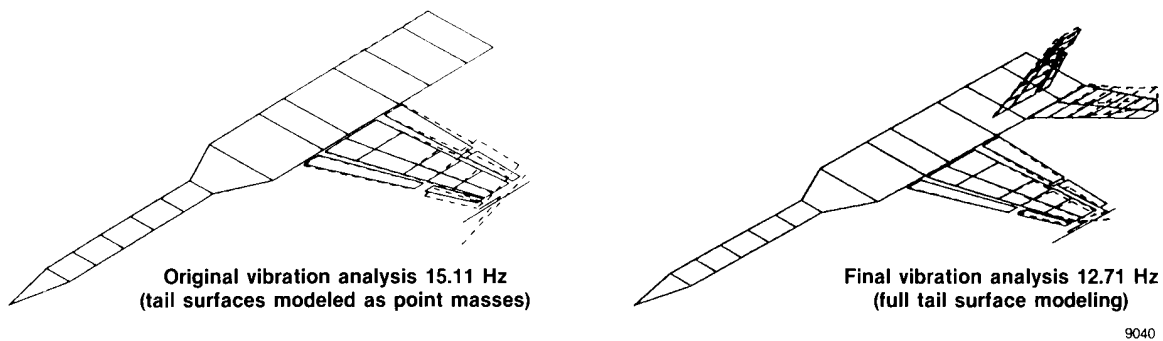


Figure 11. Analytical mode shape comparison — antisymmetric first wing torsion.

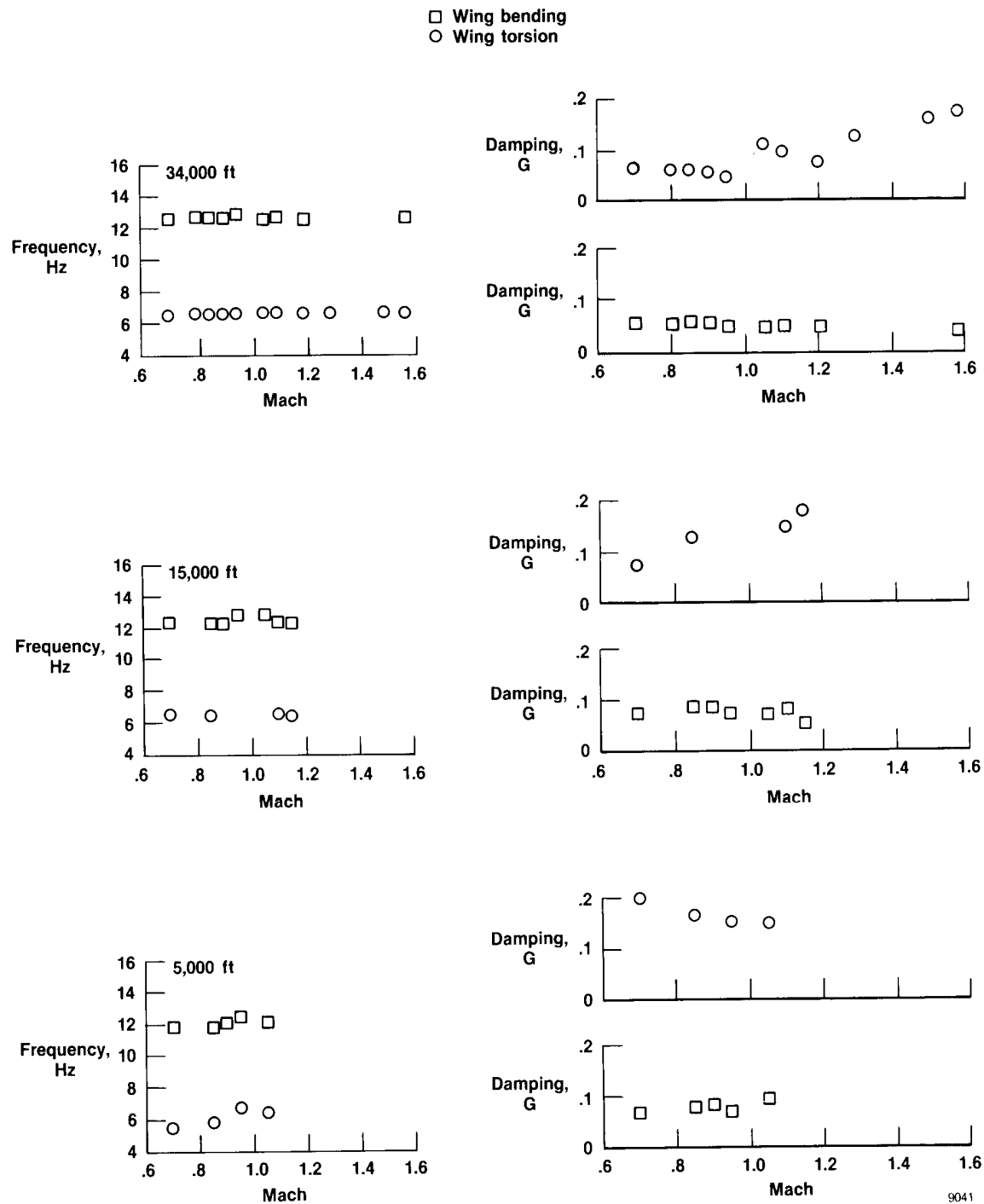


Figure 12. Flight test results for symmetric flutter mechanism.

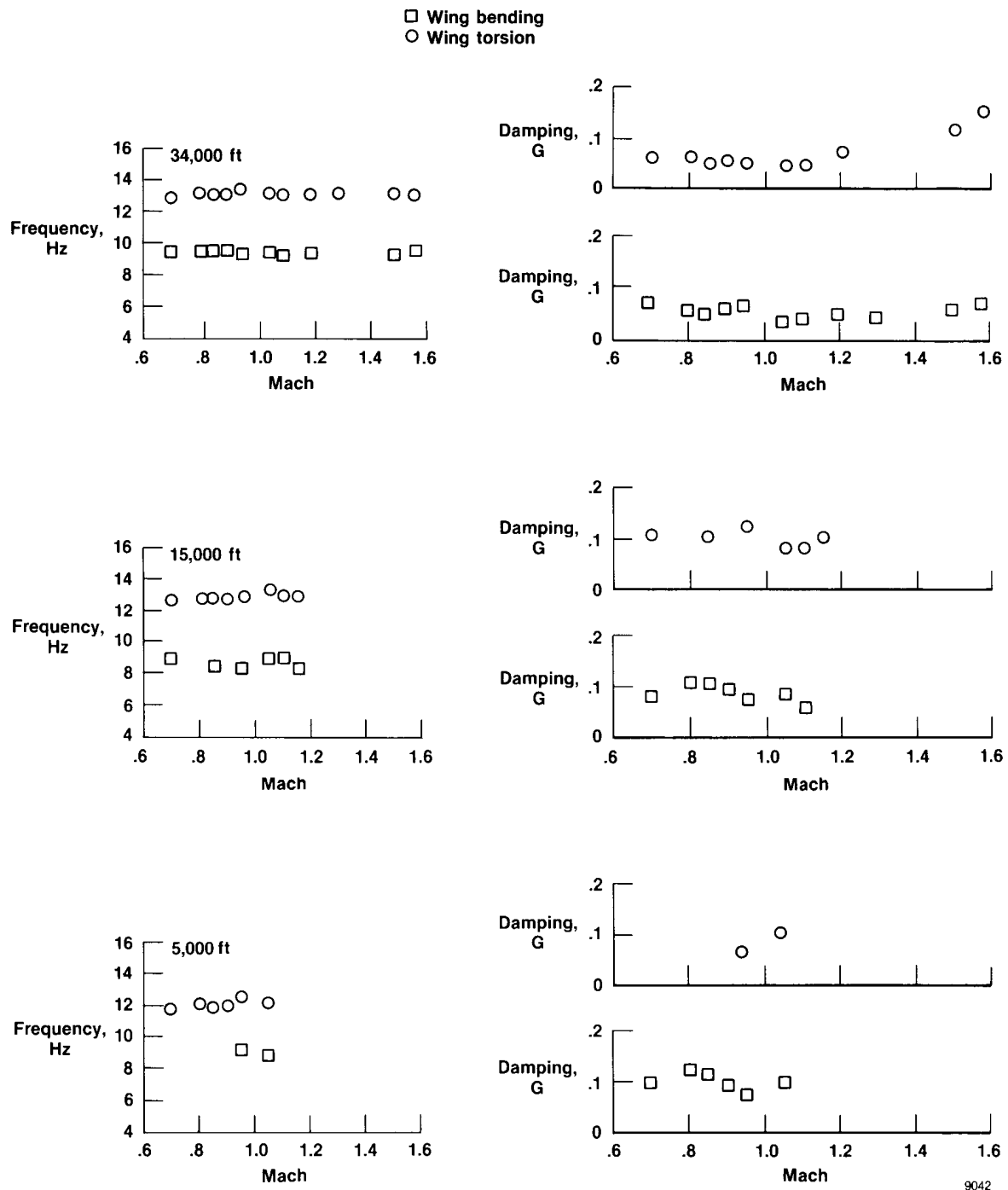


Figure 13. Flight test results for antisymmetric flutter mechanism.

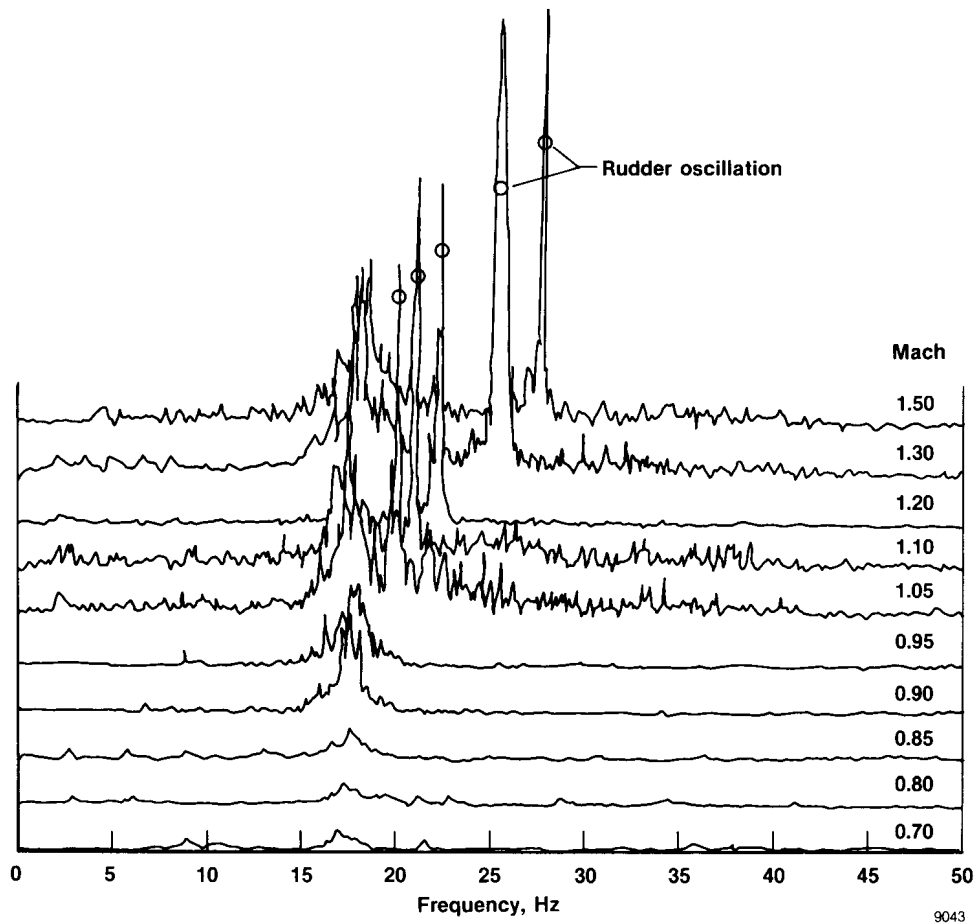


Figure 14. Vertical stabilizer data indicating rudder freeplay.

9043

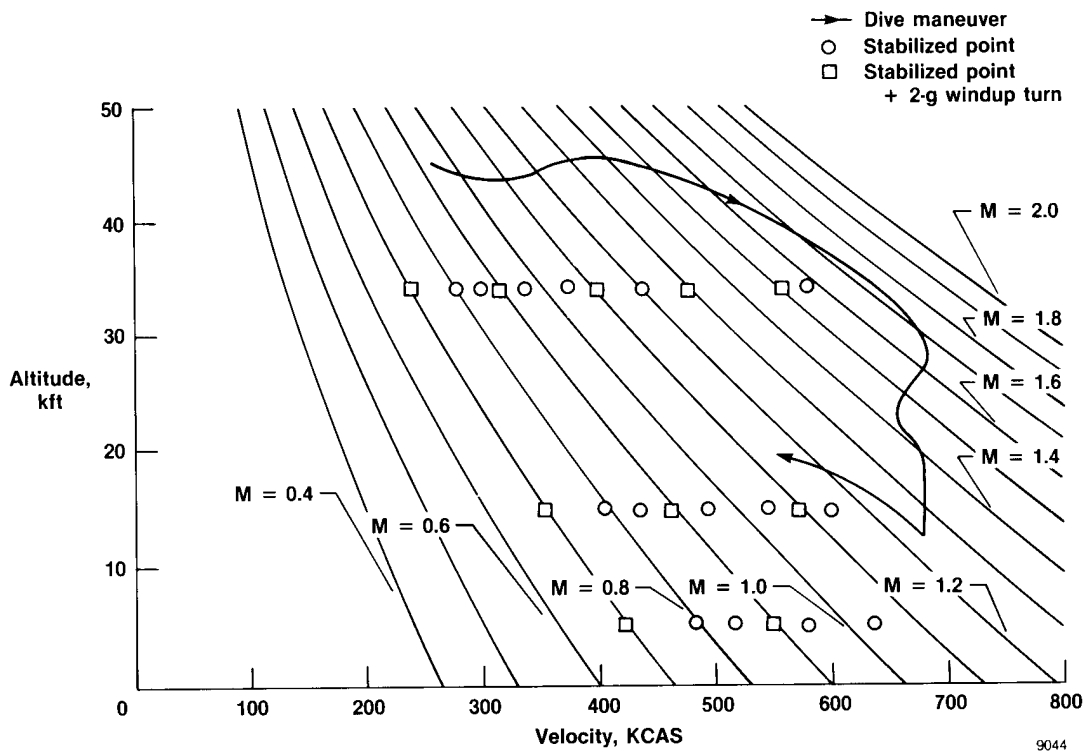


Figure 15. Completed test points.

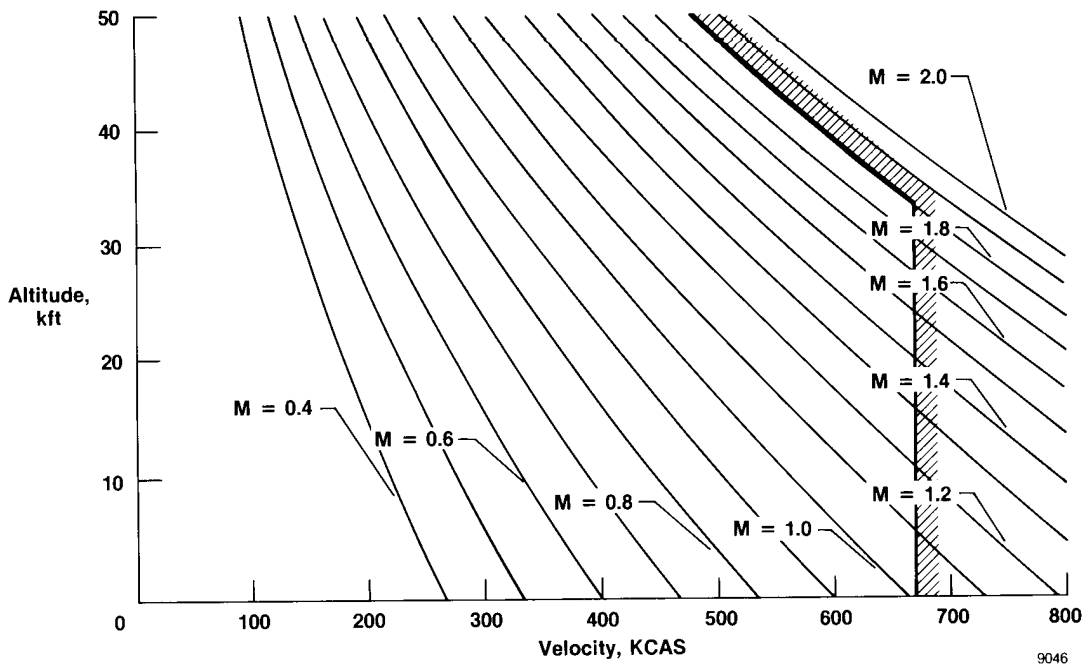


Figure 16. Cleared flight envelope.



Report Documentation Page

1. Report No. NASA TM-4148		2. Government Accession No.		3. Recipient's Catalog No.	
4. Title and Subtitle Flutter Clearance of the F-18 High-Angle-of-Attack Research Vehicle With Experimental Wingtip Instrumentation Pods			5. Report Date October 1989		
			6. Performing Organization Code		
7. Author(s) Lawrence C. Freudinger			8. Performing Organization Report No. H-1528		
			10. Work Unit No. RTOP 533-02-71		
9. Performing Organization Name and Address NASA Ames Research Center Dryden Flight Research Facility P.O. Box 273, Edwards, CA 93523-5000			11. Contract or Grant No.		
			13. Type of Report and Period Covered Technical Memorandum		
12. Sponsoring Agency Name and Address National Aeronautics and Space Administration Washington, DC 20546			14. Sponsoring Agency Code		
			15. Supplementary Notes		
16. Abstract An F-18 aircraft was modified with wingtip instrumentation pods for use in NASA's high-angle-of-attack research program. Ground vibration and flight flutter testing were performed to clear an acceptable flight envelope for the aircraft. Flight test utilized atmospheric turbulence for structural excitation; the aircraft displayed no adverse aeroelastic trends within the envelope tested. The data presented in this report include mode shapes from the ground vibration tests and estimates of frequency and damping as a function of Mach number.					
17. Key Words (Suggested by Author(s)) Flight test Flutter Ground vibration test Modal analysis			18. Distribution Statement Unclassified — Unlimited Subject category 05		
19. Security Classif. (of this report) Unclassified		20. Security Classif. (of this page) Unclassified		21. No. of pages 24	22. Price A02